IET Communications

Research Article

Peak-to-average power ratio reduction in multiple-input multiple-output orthogonal frequency-division multiple access systems using geodesic descent method

ISSN 1751-8628
Received on 13th June 2015
Revised on 15th September 2015
Accepted on 22nd October 2015
doi: 10.1049/iet-com.2015.0563
www.ietdl.org

Marko Beko[1,2] ✉, *Milica Marikj*[3], *Rui Dinis*[3,4], *Milan Tuba*[5]

[1]*Universidade Lusófona de Humanidades e Tecnologias, Campo Grande 376, 1749-024 Lisboa, Portugal*
[2]*CTS-UNINOVA, Campus da FCT/UNL, Monte de Caparica, 2829-516 Caparica, Portugal*
[3]*Dep.º de Eng.ª Electrotécnica, Faculdade de Ciências e Tecnologia, FCT, CTS-UNINOVA, Universidade Nova de Lisboa, 2829-516 Caparica, Portugal*
[4]*Instituto de Telecomunicações, Av. Rovisco Pais 1, 1049-001 Lisboa, Portugal*
[5]*Faculty of Computer Science, John Naisbitt University, Bulevar Umetnosti 29, 11070 Belgrade, Serbia*
✉ *E-mail: mbeko@uninova.pt*

Abstract: In this study, the authors consider a peak-to-average power ratio (PAPR) reduction for orthogonal frequency-division multiplexing systems based on the decomposition of the set of subcarriers in subsets of subcarriers, denoted resource blocks, each one weighted by a different complex factor. They present a new iterative sphere-geodesic descent method for obtaining these weighting factors so as to minimise the PAPR of the transmitted signals. This method, which they term geodesic descent method, efficiently makes use of the Riemannian structure of the power constraint. The authors' performance results show that the proposed technique provides good trade-off between the PAPR reduction and the bit error rate performance, for both uncoded and coded scenarios.

1 Introduction

Orthogonal frequency-division multiplexing (OFDM) schemes [1] are the key modulation for broadband wireless communications over severely time-dispersive channels. However, OFDM signals have high envelope fluctuations and high peak-to-average power ratio (PAPR), which leads to amplification difficulties since linear amplifiers with high backoff are required, which reduces the amplification efficiency [2]. Since the amplifier backoff is lower-bounded by the PAPR, it is desirable to reduce the PAPR of OFDM signals so as to improve the amplification efficiency.

Over the last decades, countless techniques were proposed to reduce the PAPR of OFDM signals from the simpler clipping techniques [3–6] to more complex techniques involving different levels of optimisation [7, 8]. Selected mapping (SLM) and partial transmit sequences are among the most popular techniques [9–11]. However, generalisation of these techniques to multiple-input multiple-output (MIMO) systems is not straightforward. Combined precoding and PAPR reduction for multiuser MIMO systems have been addressed in [12]. Siegl and Fischer introduced in [12] a combination of the simplified SLM [13] with lattice-reduction aided Tomlinson-Harashima precoding [14].

In general, the PAPR minimisation of OFDM signals is a complex optimisation problem. To overcome these difficulties, convex optimisation methods were recently proposed as an efficient tool for reducing the PAPR of OFDM signals [15–19]. Although allowing substantial complexity gains, these techniques are still too complex for practical implementations, since the number of subcarriers is usually in the order of several hundreds, which means an optimisation problem with a large number of variables.

A promising technique to reduce the optimisation complexity was proposed in [20] where an OFDM block with a large number of subcarriers is divided into resource blocks (RBs), each one with several subcarriers. A different complex weighting is assigned to each RB and these weighting factors are optimised to minimise the PAPR of the transmitted signals, either employing a constant modulus approach or a steepest descent algorithm. However, Khademi and Veen [20] considered only uncoded OFDM schemes.

In this paper, we consider the PAPR reduction of OFDM schemes and we employ RBs' weighting approach of [20]. We propose a geodesic descent method (GDM) which, in sharp contrast to [20], generates a sequence of feasible precoding weights, not requiring projections onto the feasible set and feasibility checks. Moreover, different techniques are compared taking into account frequency-selective channel and appropriate channel coding schemes.

The remainder of this paper is organised as follows. The design of precoding weights for PAPR reduction is formulated as an optimisation problem in Section 2. Our approach for solving this optimisation problem is described in Section 3. The performance results are presented in Section 4. Section 5 is concerned with the conclusions of this paper.

2 System model

Similar to [20], a MIMO OFDM/A downlink scenario with one base station using M_t antennas is considered. An N-subcarrier OFDM block is transmitted from each antenna. The N subcarriers are divided into three disjoint sets: data subcarriers, pilot subcarriers and guard subcarriers, with cardinalities N_d, N_p and N_g, respectively, so that $N_\mathrm{d}+N_\mathrm{p}+N_\mathrm{g}=N$. To prevent intersymbol interference at the receiver caused by multipath delay spread in the radio channel, the $N_\mathrm{d}+N_\mathrm{p}$ useful subcarriers are surrounded by two guard bands with zero energy. Each RB contains pilot subcarriers which are used for synchronisation and channel estimation. The data and pilot subcarriers are grouped into M RBs, each of them comprising $N_b=(N-N_\mathrm{g})/M$ subcarriers.

In what follows, we present the MIMO transmit model in the frequency domain. Without loss of generality, in the remainder of this paper, only a single time block is considered. The transmit sequence in the qth RB, $\boldsymbol{X}_{(q)}$, is given by $\boldsymbol{X}_{(q)}=\boldsymbol{W}_{(q)}^{\mathrm{H}}\boldsymbol{D}_{(q)}$, where

input: The vector $\boldsymbol{s}_{(0)}$;

step 1) Determine the initial value of the objective function, $\text{cost} = \left\| \boldsymbol{A}\left(\boldsymbol{A}^H\boldsymbol{A}\right)^{-1/2}\boldsymbol{s}_{(0)} \right\|_\infty^2$;

step 2) Initialise ϵ. Set $k=0$;

step 3) Construct the vector $\tilde{\boldsymbol{s}}_{(k)} = \begin{bmatrix} \Re\{\boldsymbol{s}_{(k)}\} \\ \Im\{\boldsymbol{s}_{(k)}\} \end{bmatrix}$;

step 4) Determine z, the number of entries of the vector $\boldsymbol{A}\left(\boldsymbol{A}^H\boldsymbol{A}\right)^{-1/2}\boldsymbol{s}_{(k)}$, such that $f_i\left(\boldsymbol{s}_{(k)}\right) = \left|\left(\boldsymbol{A}\left(\boldsymbol{A}^H\boldsymbol{A}\right)^{-1/2}\boldsymbol{s}_{(k)}\right)_i\right|^2$ falls into the interval $[\text{cost}-\epsilon, \text{cost}]$, i.e. f_i attains the maximum. These entries are called the active ones;

step 5) Determine the gradient, $\nabla f_{i_a}\left(\boldsymbol{s}_{(k)}\right)$, for every active entry i_a, where $1 \le i_a \le MM_t$, $a = 1, 2, \ldots, z$;

step 6) Construct the gradient matrix

$$\boldsymbol{G} = \begin{bmatrix} \nabla^T f_{i_1}\left(\boldsymbol{s}_{(k)}\right) \\ \vdots \\ \nabla^T f_{i_z}\left(\boldsymbol{s}_{(k)}\right) \end{bmatrix}_{z\times 2MM_t};$$

step 7) Solve the linear program

$$(\boldsymbol{d}^*, s^*) = \underset{\substack{\boldsymbol{G}\boldsymbol{d} \le s\mathbf{1}_{z\times 1} \\ \boldsymbol{d}^T\tilde{\boldsymbol{s}}_{(k)} = 0 \\ -\mathbf{1}_{2MM_t\times 1} \le \boldsymbol{d} \le +\mathbf{1}_{2MM_t\times 1}}}{\arg\min}\ s;$$

step 8) If $s^* \ge 0$, Go to Step (15);

step 9) Initialise $\beta = 0.9$, $c = 0$, $c_{max} = 400$ and $t = 1$;

step 10) Construct the geodesic

$$\tilde{\boldsymbol{s}}_{(k)}(t) = \tilde{\boldsymbol{s}}_{(k)}\cos(||\boldsymbol{d}^*||t) + \frac{\boldsymbol{d}^*}{||\boldsymbol{d}^*||}\sin(||\boldsymbol{d}^*||t);$$

step 11) Construct $\boldsymbol{s}_{(k)}(t)$ out of $\tilde{\boldsymbol{s}}_{(k)}(t)$; Determine the (temporary) value of the objective function, $\text{tempcost} = \left\| \boldsymbol{A}\left(\boldsymbol{A}^H\boldsymbol{A}\right)^{-1/2}\boldsymbol{s}_{(k)}(t) \right\|_\infty^2$;

step 12) If tempcost < cost, then Increment k, Set cost = tempcost, $\boldsymbol{s}_{(k)} = \boldsymbol{s}_{(k-1)}(t)$, If $k \le k_{max}$ Return to Step (3), else Go to Step (15);

step 13) Increment c, update $t = \beta^c$;

step 14) If $c \le c_{max}$, Return to Step (10);

step 15) Set $\boldsymbol{s} = \boldsymbol{s}_{(k)}$; Return the vector $\boldsymbol{s}$;

output: The vector $\boldsymbol{s}$;

Fig. 1 *Geodesic descent method*

$\boldsymbol{W}_{(q)}$ is an orthonormal $M_t \times M_t$ beamforming matrix and $\boldsymbol{D}_{(q)}$ is a $M_t \times N_b$ data matrix. Let $\boldsymbol{X} = [\boldsymbol{X}_{(1)}, \boldsymbol{X}_{(2)}, \ldots, \boldsymbol{X}_{(M)}]$ be the beamformed data matrix in the frequency domain. Then, we can write

$$\boldsymbol{X} = \boldsymbol{W}^{\mathrm{H}}\boldsymbol{D},$$

where $\boldsymbol{W} = \left[\boldsymbol{W}_{(1)}^{\mathrm{H}}, \boldsymbol{W}_{(2)}^{\mathrm{H}}, \ldots, \boldsymbol{W}_{(M)}^{\mathrm{H}}\right]^{\mathrm{H}}$ is the beamforming matrix and $\boldsymbol{D} \in \mathbb{C}^{MM_t \times N}$ is a block-diagonal matrix with $\boldsymbol{D}_{(q)}$ at the position of the qth block. See [20] for more details. The corresponding time-domain MIMO-OFDM transmit data model can be obtained by taking the inverse fast Fourier transform (IFFT), i.e.

$$\boldsymbol{Y} = \boldsymbol{X}\boldsymbol{F}^{\mathrm{H}} = \boldsymbol{W}^{\mathrm{H}}\boldsymbol{B},$$

where $\boldsymbol{F}^{\mathrm{H}} \in \mathbb{C}^{N\times N}$ denotes the IFFT matrix, $\boldsymbol{B} = \boldsymbol{D}\boldsymbol{F}^{\mathrm{H}}$ and $\boldsymbol{Y}$ contains the transmit OFDM sequences [20].

The PAPR is defined as the ratio of the peak power of the signal to its average power. Mathematically, the PAPR of an OFDM block $\boldsymbol{Y}$

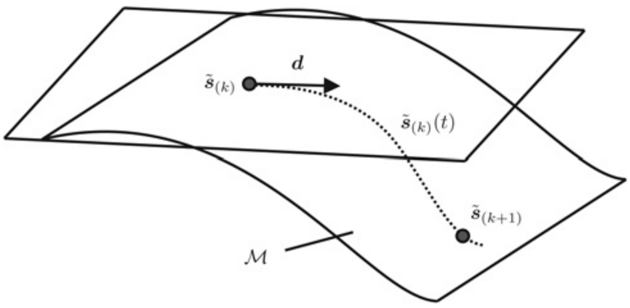

Fig. 2 *Geodesic $\tilde{\mathbf{s}}_{(k)}(t)$ and a tangent vector $\boldsymbol{d}$ on a smooth manifold $\mathcal{M}$. Tangent vector lies in the tangent space at a point $\tilde{\mathbf{s}}_{(k)}$*

can be written as

$$\mathrm{PAPR}(\boldsymbol{Y}) = \alpha N_t \frac{||\mathrm{vec}(\boldsymbol{Y})||_\infty^2}{||\mathrm{vec}(\boldsymbol{Y})||^2}, \tag{1}$$

where vec ($\boldsymbol{Y}$) stacks all columns of $\boldsymbol{Y}$ on the top of each other (from left to right), $N_t = NM_t$ and α is defined as the average transmit power per sample. Actually, αN_t denotes the total power in the data matrix $\boldsymbol{D}$ [20].

Precoding is an effective way for reducing the PAPR [15, 19, 20]. The idea behind the approaches in [15, 19, 20] is to design a diagonal precoding matrix $\boldsymbol{\Omega}$ to transform $\boldsymbol{Y}$ to a new signal $\boldsymbol{T}$ with lower PAPR. More precisely, the precoding matrix $\boldsymbol{\Omega} \in \mathbb{C}^{MM_t \times MM_t}$ is applied to the data matrix $\boldsymbol{D}$ to generate the new MIMO-OFDM transmit matrix

$$\boldsymbol{T} = \boldsymbol{W}^{\mathrm{H}} \boldsymbol{\Omega} \boldsymbol{D} \boldsymbol{F}^{\mathrm{H}}.$$

If $\boldsymbol{w} = \mathrm{diag}(\boldsymbol{\Omega})$, the PAPR reduction problem is formulated as

$$\underset{\boldsymbol{w} \in \mathbb{C}^{MM_t}}{\text{minimise}} \quad ||\mathrm{vec}(\boldsymbol{T})||_\infty^2 \tag{2}$$

subject to

$$||\mathrm{vec}(\boldsymbol{T})||^2 = \alpha N_t. \tag{3}$$

The operator diag($\boldsymbol{\Omega}$) creates a vector containing the elements of the principal diagonal of $\boldsymbol{\Omega}$. It is not difficult to show that the PAPR reduction problems (2) and (3) are equivalent to

$$\underset{\boldsymbol{w} \in \mathbb{C}^{MM_t}}{\text{minimise}} \quad ||\boldsymbol{A}\boldsymbol{w}||_\infty^2 \tag{4}$$

subject to

$$\|\boldsymbol{A}\boldsymbol{w}\|^2 = \alpha N_t, \tag{5}$$

where $\boldsymbol{A} = (\bar{\boldsymbol{B}} \circ \boldsymbol{W})^{\mathrm{H}}$, $\bar{\boldsymbol{B}}$ denotes the complex conjugate of $\boldsymbol{B}$ and $\circ$ denotes the column-wise Kronecker product. For more details see [20]. It is straightforward to see that the optimisation problems (4) and (5) can be rewritten as

$$\underset{\boldsymbol{s} \in \mathbb{C}^{MM_t}}{\text{minimise}} \quad \left|\left|\boldsymbol{A}(\boldsymbol{A}^{\mathrm{H}}\boldsymbol{A})^{-1/2}\boldsymbol{s}\right|\right|_\infty^2 \tag{6}$$

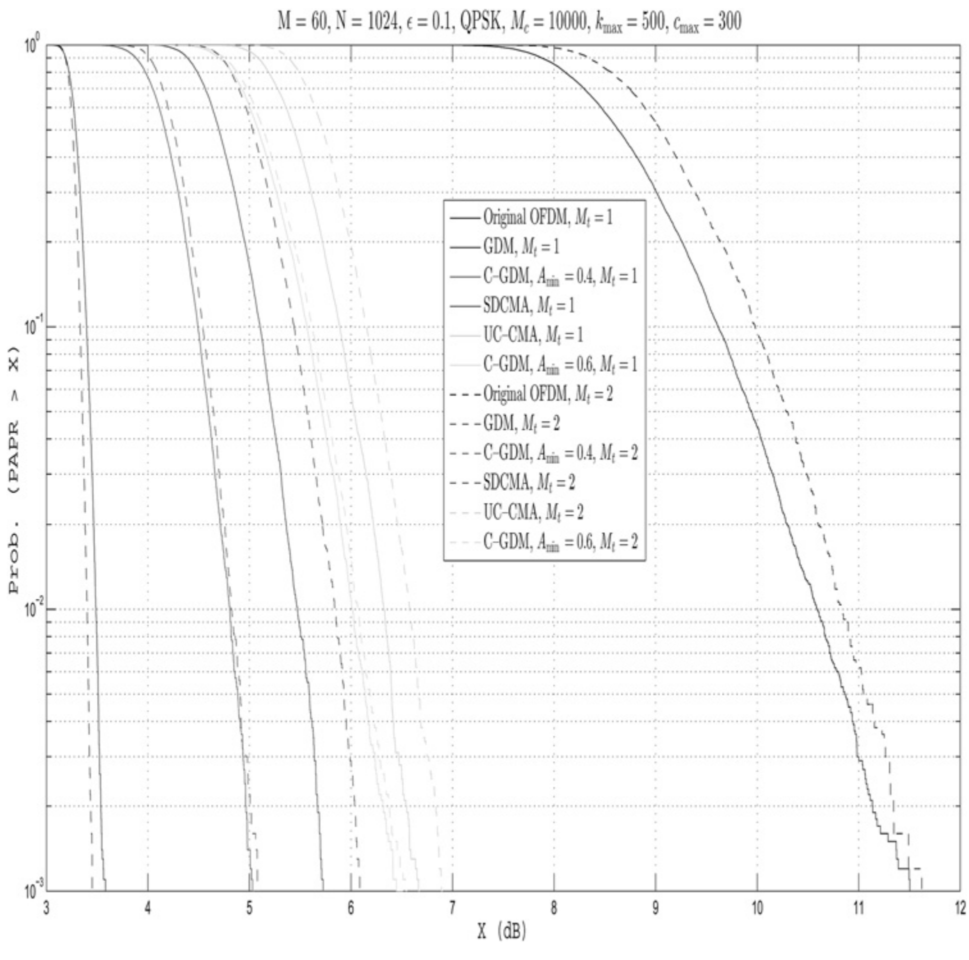

Fig. 3 *CCDF of the PAPR with different algorithms*

IET Commun., 2016, Vol. 10, Iss. 2, pp. 212–218

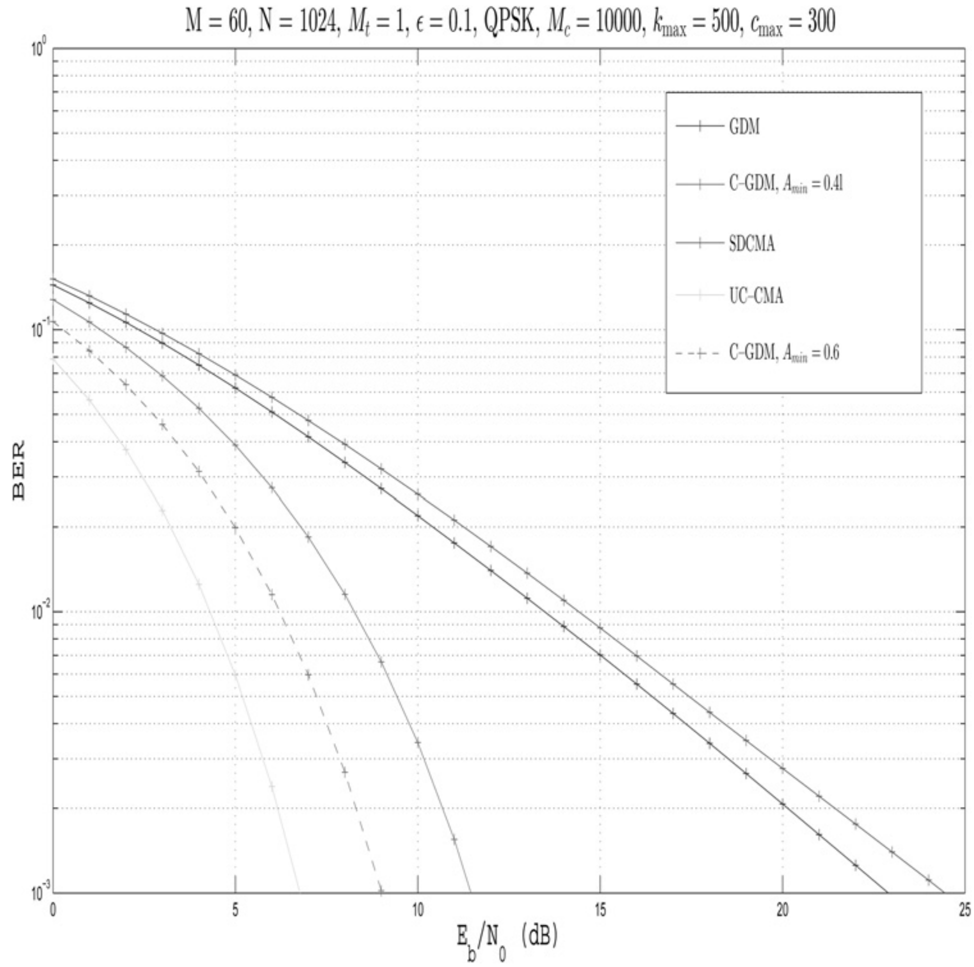

Fig. 4 *Uncoded BER performance for an AWGN channel*

subject to

$$\|s\|^2 = \alpha N_t, \tag{7}$$

where $s = (A^H A)^{1/2} w$. The PAPR optimisation frameworks (6) and (7) result in a non-convex optimisation problem since the constraint (7) is non-convex [21]. As most non-convex problems, (6) and (7) are NP-hard and, hence, difficult to solve [21].

3 Proposed GDM

In this section, we present an iterative method to generate precoding vectors which transform the OFDM symbols in Y to a signal T with lower PAPR. Without loss of generality, in this section, for the sake of presentation, we set $\alpha N_t = 1$. The problem defined in (6) and (7) is a high-dimensional, non-linear, non-convex and non-smooth min–max optimisation problem. Problems (6) and (7) require the optimisation of a non-smooth function over the smooth manifold S^{2MM_t-1} (the symbol S^{n-1} denotes the unit sphere in $\mathbb{R}^n$). The method, which we call a geodesic descent method, is explained in Fig. 1 in more detail.

Let $s_{(k)}$ be the kth iterate (the initialisation $s_{(0)}$ is generated randomly). Note that the power constraint $\|s_{(k)}\|^2 = 1$, can be equivalently written as

$$\|\tilde{s}_{(k)}\|^2 = 1,$$

where

$$\tilde{s}_{(k)} = \begin{bmatrix} \Re\{s_{(k)}\} \\ \Im\{s_{(k)}\} \end{bmatrix} \in \mathbb{R}^{2MM_t},$$

and $\Re\{\cdot\}$ and $\Im\{\cdot\}$ denote the real and imaginary parts of a complex number, respectively. In step 3, $\tilde{s}_{(k)}$ is used to construct the vector $\tilde{s}_{(k)}$. In step 4, the index set $\mathcal{A}$ of 'active' entries i is identified, i.e. $\mathcal{A} = \{i\text{: cost} - f_i \le \epsilon\}$, where $\text{cost} = ||A(A^H A)^{-1/2} s_{(k)}||_\infty^2$, $f_i(s_{(k)}) = |(A(A^H A)^{-1/2} s_{(k)})_i|^2$, $(p)_i$ denotes the ith entry of the vector p and ϵ is arbitrary small positive constant. In step 7, we check if there is an descent direction d simultaneously for all functions f_i with $i \in \mathcal{A}$. If it exists d such that $\nabla^T f_{i_a}(s_{(k)}) d < 0$, for $1 \le i_a \le MM_t$, $a = 1, 2, \ldots, z$, where z denotes the number of active functions f_i, we can try to improve the objective function locally. To solve the optimisation problem in step 7 we need to determine the gradient ∇f_{i_a}. In the Appendix, we give its respective expression. This descent direction d is searched within the tangent space at $\tilde{s}_{(k)}$, and consists in solving a linear program. To ensure that d belongs to the tangent space, the constraint $d^T \tilde{s}_{(k)} = 0$ in step 7 is introduced. The constraint $-\mathbf{1}_{2MM_t \times 1} \le d \le +\mathbf{1}_{2MM_t \times 1}$ bounds the solution of the linear program in step 7. If there is no such descent direction, the algorithm stops. Otherwise, an Armijo search along the geodesic $\tilde{s}_{(k)}(t)$ which originates from $\tilde{s}_{(k)}$ in the direction d is performed; see Fig. 2. This search determines $\tilde{s}_{(k+1)}$ and the loop is repeated.

A geodesic is nothing, but the analogue of a straight line in the Euclidean space to a curved manifold [22]. In other words, a geodesic is the shortest path between two points on a curved surface. The constant ϵ in step 2 determines the complexity of the optimisation problem in step 7; if ϵ is too small the convergence of the GDM is slow in general, whereas too big ϵ implies increased complexity of the linear program.

From the expression for the geodesic in step 10, it is easy to see that we move along the surface of S^{2MM_t-1}, i.e. $\|\tilde{s}_{(k)}(t)\|^2 = 1$, for $\forall k$ and $\forall t$. Hence, in sharp contrast to [20], a sequence of feasible precoding weights is generated, not requiring projections onto the feasible set and feasibility checks.

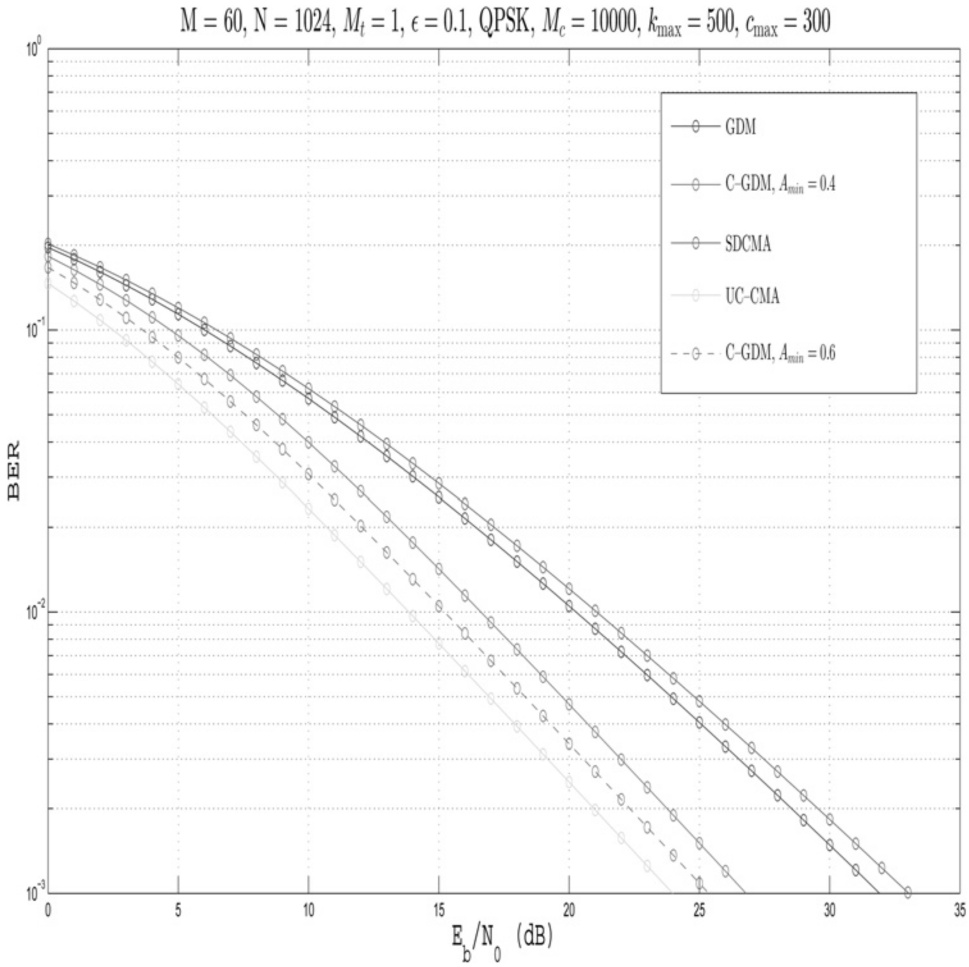

Fig. 5 *Uncoded BER performance for a frequency selective fading channel*

4 Performance results

In this section, computer simulations are performed in order to compare the performance of the new approach with the state-of-the-art RB's weighting approaches [20]. We focus on a 10 MHz WiMAX system [23], although our techniques could easily be extended to other scenarios. In this system, a RB extends across 2 OFDM symbols in time, containing 24 data symbols and 4 pilots. The number of RBs is $M = 60$, the number of subcarriers is $N = 1024$, the number of guard subcarriers is $N_g = 184$ (92 at each end of the band) and, consequently, $N_b = 14$. Unless stated otherwise, the data and pilot subcarriers are generated from quadrature phase shift keying and the oversampling factor is assumed to be 4.

We use the complementary cumulative density function (CCDF) or the PAPR to evaluate the PAPR-reduction potential of different techniques. This CCDF is the probability that an arbitrary OFDM block has PAPR greater than a given threshold. The new algorithms described above, denoted here by 'GDM', will be compared with the steepest descent constant modulus algorithm, denoted here by 'SDCMA' and unit circle constant modulus algorithm, denoted here by 'UC–CMA', both proposed in [20]. The number of iterations, $k_{\max}$, is set to 500 and ϵ is set to 0.1. For each block, the beamforming matrices $\boldsymbol{W}_{(q)}$, $q = 1, \ldots, M$, are chosen as the right singular vectors of randomly generated channel matrices. We also present the performance of the new algorithm with clipping, called here 'C–GDM', for different values of the clipping level $A_{\min}$. In this case, if the absolute value of $(\boldsymbol{w})_i$ is smaller than $A_{\min}$, it is set to $A_{\min}$, while maintaining the phase (clearly, having $A_{\min} = 0$ reduces to the 'unclipped GDM').

Fig. 3 shows the PAPR's CCDF for different algorithms. From Fig. 3, we can see that all four methods reduce the PAPR. We also observe that GDM outperforms significantly the existing approaches. Furthermore, when compared to SDCMA and UC–CMA, we note that GDM has sharper cutoff, demonstrating reduced variation in the PAPR of our optimised OFDM blocks. Fig. 3 also presents the effect of the number of transmit antennas on the PAPR performance. We observe that the PAPR performance of our approach, in huge contrast to SDCMA and UC–CMA, improves with the increase of M_t. This implies that the new approach exploits additional degrees of freedom offered by an extra transmit antenna more efficient than the existing approaches. Fig. 3 further illustrates the effect of the clipping on the PAPR performance of the new approach. As expected, when the clipping is performed, the PAPR increases as the clipping level $A_{\min}$ increases; an increase of $A_{\min}$ from 0 to 0.4 and 0.6 leads to increases in the PAPR of 1.5 and 3 dB, respectively.

Clearly a proper selection of the weights $\boldsymbol{w}$ allows substantial gains in the PAPR. However, if the absolute value of $(\boldsymbol{w})_i$ have fluctuations this leads to performance degradation, in a similar way to channel fading. To evaluate this performance degradation we study the bit error rate (BER) with the different PAPR-reduction techniques.

Figs. 4 and 5 show the BER performance with different PAPR-reduction techniques for both ideal AWGN and frequency-selective multipath Raleigh fading channels. The BER values are expressed as a function of E_b/N_0, where E_b denotes the average bit energy and N_0 is the one-sided power spectral density of the noise component. As expected, the performance is worse when we have fluctuations on the absolute value of $(\boldsymbol{w})_i$ (i.e. for our GDM algorithms and the SDCMA) than conventional OFDM and UC–CMA (which have identical performance). In fact, the BER of GDM and SDCMA in AWGN channels has a behaviour similar to the BER of conventional OFDM and UC–CMA in frequency selective fading channels. By performing the clipping in the absolute value of $(\boldsymbol{w})_i$ we reduce their 'inherent fades', improving the BER performance (the higher the clipping level the better the

IET Commun., 2016, Vol. 10, Iss. 2, pp. 212–218

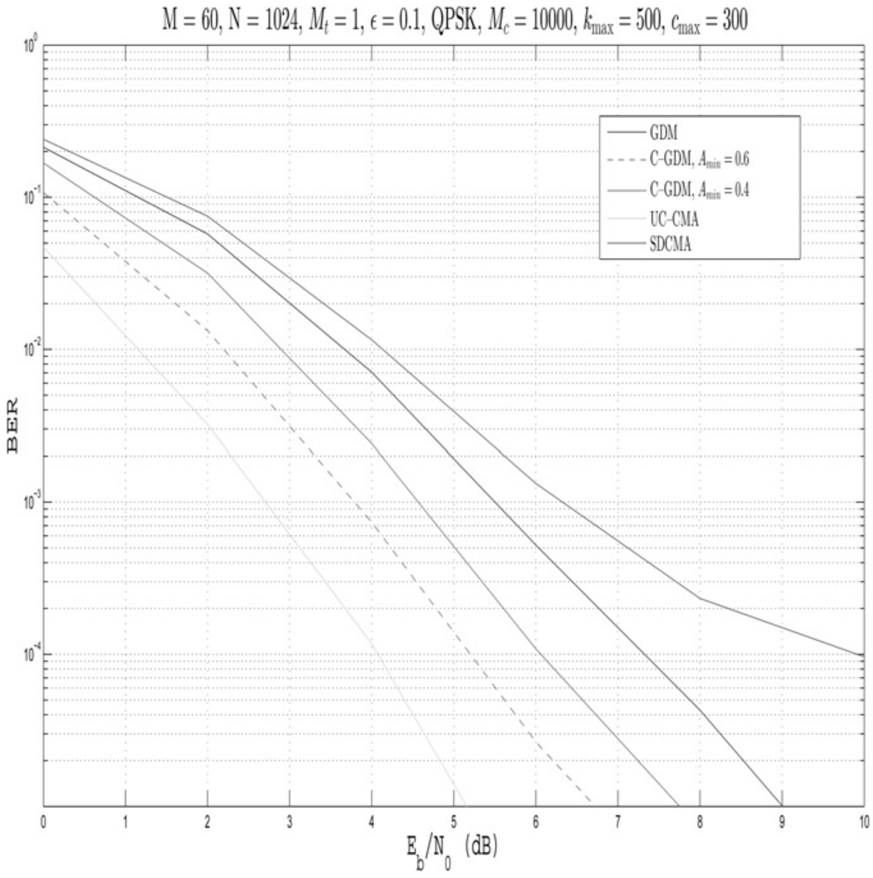

Fig. 6 *Coded BER performance for a frequency selective fading channel*

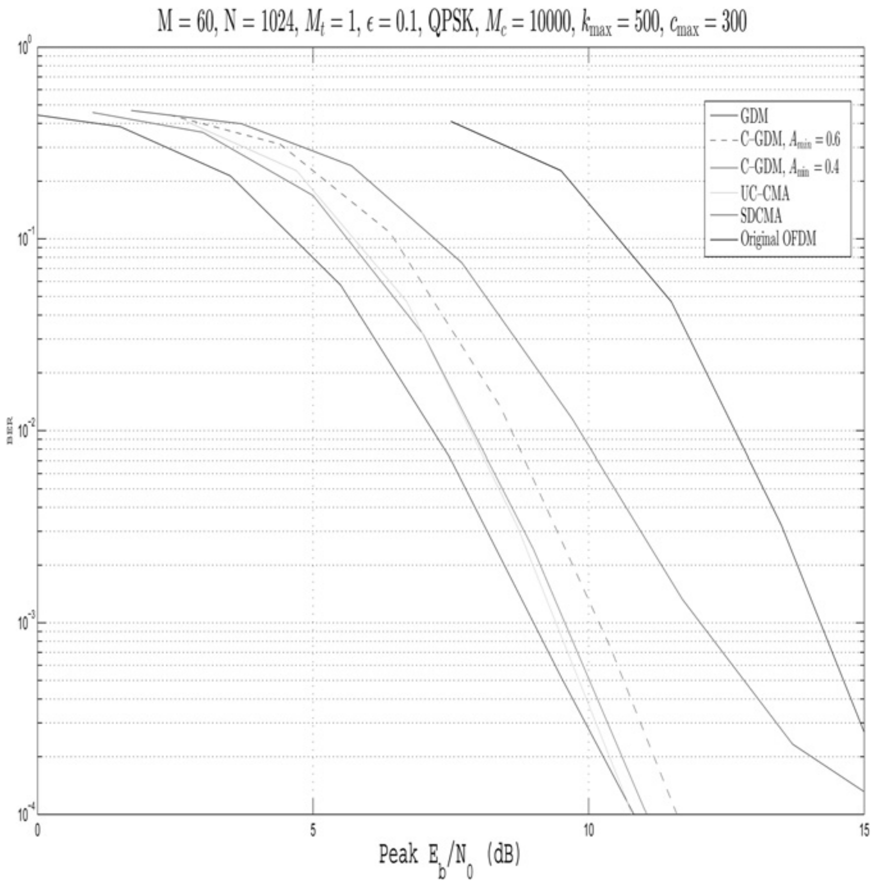

Fig. 7 *As in Fig. 6, but as a function of the peak E_b/N_0*

performance, although at the expense of increased PAPR, as shown in Fig. 3). Actually, the situation is more serious than conventional fading effects, since the equivalent fading is the combined effects of 'inherent fading' effects associated with the weighting and channel fading.

It is well-known that appropriate channel coding schemes are very effective to improve the performance of conventional OFDM schemes in frequency selective fading channels. Therefore, we compared different PAPR-reduction techniques in coded conditions. We considered a rate-1/2, 64-state convolutional code, although similar conclusions could be drawn with other coding schemes.

Fig. 6 shows the coded BER performance for frequency selective fading channels with different PAPR-reduction techniques. Clearly, our GDM methods outperform SDCMA for all values of $A_{\min}$ (even without clipping). As expected, the BER performance improves as we increase $A_{\min}$, approaching the performance of conventional OFDM and UC–CMA.

A simple way of combining the PAPR values on the BER performance is by expressing the BER as a function of the 'peak E_b/N_0', given by 'PAPR + E_b/N_0 (dB)'. These results are depicted in Fig. 7. From this figure, it is clear that GDM and UC–CMA have similar performances, significantly outperforming conventional OFDM and SDCMA, although the PAPR values of GDM are much lower than UC–CMA, which simplifies the power amplification.

Regarding the computational complexity analysis, the situation is the following. Whereas the computational complexity of SDCMA is $O(M)$, the computational complexity of the method in [19] is $O(M^3)$; see [19, 20], respectively, for the exact expressions. Hence, the computational complexity of GDM is somewhat higher than that of SDCMA, since GDM involves solving a linear program. At the same time, the computational complexity of GDM is lower than that of the method proposed in [19], since the latter involves solving a convex quadratic optimisation problem.

5 Conclusions

We have addressed the PAPR reduction problem in OFDM systems. The OFDM blocks are divided into several RBs with different weighting factors which are selected to minimise the PAPR. We formulated the PAPR minimisation problem as a constrained non-convex optimisation problem. This problem was addressed by a geodesic descent iterative method which efficiently exploits the Riemannian structure of the constraint. The simulation results showed that the new method outperforms significantly the existing ones in terms of PAPR performance, thus providing a lower bound on the achievable PAPR performance, while at the same time, the proposed method replicates the existing methods in terms of the overall BER performance. This shows the relevance of the PAPR reduction tool presented herein.

6 Acknowledgments

This work was partially supported by Fundação para a Ciência e a Tecnologia under Projects PTDC/EEI-TEL/2990/2012–ADIN, EXPL/EEI-TEL/1582/2013–GLANC, UID/EEA/50008/2013, UID/EEA/00066/2013, PEst-OE/EEI/UI0066/2014 and EXPL/EEI-TEL/0969/2013–MANY2COMWIN, COPWIN PTDC/EEI-TEL/1417/2012 and PTDC/EEITEL/6308/2014-HAMLeT, as well as the grant SFRH/BPD/108232/2015 and 2008 Post-Doctoral Research grant. This work was also supported by Ministry of Education and Science of Republic of Serbia, Grant No. III-44006.

7 References

1 Cimini, L.: 'Analysis and simulation of a digital mobile channel using orthogonal frequency division multiplexing', *IEEE Trans. Commun.*, 1985, **33**, (7), pp. 665–675
2 Dinis, R., Gusmão, A.: 'A new class of signal processing schemes for bandwidth-efficient OFDM transmission with low envelope fluctuation'. Proc. IEEE Vehicular Technol. Conf., Rhodes, May 2001, pp. 658–662
3 Li, X., Cimini, L.J. Jr.: 'Effects of clipping and filtering on the performance of OFDM', *IEEE Commun. Lett.*, 1998, **2**, (5), pp. 131–133
4 Dinis, R., Gusmão, A.: 'On the performance evaluation of OFDM transmission using clipping techniques'. Proc. IEEE Vehicular Technol. Conf., Amsterdam, September 1999, pp. 2923–2928
5 Armstrong, J.: 'Peak-to-average power reduction for OFDM by repeated clipping and frequency domain filtering', *Electron. Lett.*, 2002, **38**, (5), pp. 246–247
6 Dinis, R., Gusmão, A.: 'A class of nonlinear signal processing schemes for bandwidth-efficient OFDM transmission with low envelope fluctuation', *IEEE Trans. Commun.*, 2004, **52**, (11), pp. 2009–2018
7 Müller, S., Bräuml, R., Fisscher, R., *et al.*: 'OFDM with reduced peak-to-average power ratio by multiple signal representation', *Ann. Telecommun.*, 1997, **52**, (1–2), pp. 58–67
8 Krongold, B., Jones, L.: 'An active-set approach for OFDM PAR reduction via tone reservation', *IEEE Trans. Signal Process.*, 2004, **52**, (2), pp. 495–509
9 Han, S.H., Lee, J.H.: 'An overview of peak-to-average power ratio reduction techniques for multicarrier transmission', *IEEE Wirel. Commun. Mag.*, 2005, **12**, (12), pp. 56–65
10 Cimini, L. Jr., Sollenberger, N.: 'Peak-to-average power reduction of an OFDM signal using partial transmit sequences', *IEEE Commun. Lett.*, 2000, **4**, (3), pp. 86–88
11 Muller, S., Huber, J.: 'OFDM with reduced peak-to-average power ratio by optimum combination of partial transmit sequences', *Electron. Lett.*, 1997, **33**, (5), pp. 368–369
12 Siegl, C., Fischer, R.F.: 'Selected basis for PAR reduction in multi-user downlink scenarios using lattice-reduction-aided precoding', *EURASIP J. Adv. Signal Process.*, 2011, **2011**, (17), pp. 1–11
13 Baek, M.-S., Kim, M.-J., You, Y.-H., *et al.*: 'Semi-blind channel estimation and PAR reduction for MIMO-OFDM system with multiple antennas', *IEEE Trans. Broadcast.*, 2004, **50**, (4), pp. 414–424
14 Windpassinger, C., Fischer, R.F.H., Huber, J.B.: 'Lattice-reduction-aided broadcast precoding', *IEEE Trans. Commun.*, 2004, **52**, (12), pp. 2057–2060
15 Khademi, S., Svantesson, T., Viberg, M., *et al.*: 'Peak-to-average- power-ratio (PAPR) reduction in WiMAX and OFDM/A systems', *EURASIP J. Adv. Signal Process.*, 2011, **2011**, (38), pp. 1–18
16 Aggarwal, A., Meng, T.: 'Minimizing the peak-to-average power ratio of OFDM signals using convex optimization', *IEEE Trans. Signal Process.*, 2006, **5**, (8), pp. 3099–3110
17 Wang, Y.-C., Wang, J.-L., Yi, K.-C., *et al.*: 'PAPR reduction of OFDM signals with minimized EVM via semidefinite relaxation', *IEEE Trans. Veh. Technol.*, 2011, **60**, (9), pp. 4662–4667
18 Beko, M., Dinis, R., Šendelj, R.: 'Peak reduction in OFDM using second-order cone programming relaxation', *EURASIP J. Adv. Signal Process.*, 2014, **2014**, (130), pp. 1–10
19 Khademi, S., van der Veen, A.-J., Svantesson, T.: 'Precoding technique for peak-to-average-power-ratio (PAPR) reduction in MIMO OFDM/A systems'. IEEE Int. Conf. Acoustics, Speech and Signal Processing, Kyoto, March 2012, pp. 3005–3008
20 Khademi, S., Veen, A.: 'Constant modulus algorithm for peak-to-average power ratio (PAPR) reduction in MIMO OFDM/A', *IEEE Signal Proc. Lett.*, 2013, **20**, (5), pp. 531–534
21 Boyd, S., Vandenberghe, L.: 'Convex optimization' (Cambridge University Press, 2004)
22 Edelman, A., Arias, T.A., Smith, S.T.: 'The geometry of algorithms with orthogonality constraints', *SIAM J. Matrix Anal. Appl.*, 1998, **20**, (2), pp. 303–353
23 Wang, J., Lan, Z., Funada, R., *et al.*: 'On scheduling and power allocation over multiuser MIMO-OFDMA: Fundamental design and performance evaluation WiMAX systems'. Proc. IEEE Int. Symp. Personal, Indoor and Mobile Radio Communications, Tokyo, September 2009, pp. 2752–2756
24 Magnus, J.R., Neudecker, H.: 'Matrix differential calculus with applications in statistics and econometrics' (John Wiley & Sons, 1999, Revised edn.)

8 Appendix: calculating gradients

In this section, we calculate gradient to be used in step 7. Although the function f_i assumes complex valued entries, i.e. f_i: $\mathbb{C}^{MM_t} \to \mathbb{R}$, $f_i(\boldsymbol{s}_{(k)}) = |(\boldsymbol{A}(\boldsymbol{A}^{\mathrm{H}}\boldsymbol{A})^{-1/2}\boldsymbol{s}_{(k)})_i|^2$, we shall treat f_i as a function of the real and imaginary components of $\boldsymbol{s}_{(k)}$, i.e.

$$f_i: \mathbb{R}^{MM_t} \times \mathbb{R}^{MM_t} \to \mathbb{R},$$

$$f_i\left(\Re\{\boldsymbol{s}_{(k)}\}, \Im\{\boldsymbol{s}_{(k)}\}\right) = \left|\left(\boldsymbol{A}\left(\boldsymbol{A}^{\mathrm{H}}\boldsymbol{A}\right)^{-1/2}\boldsymbol{s}_{(k)}\right)_i\right|^2.$$

It is straightforward to show that f_i can be equivalently written as $f_i(\boldsymbol{s}_{(k)}) = \boldsymbol{s}_{(k)}^{\mathrm{H}}\widetilde{\boldsymbol{A}}_i\boldsymbol{s}_{(k)}$, where

$$\widetilde{\boldsymbol{A}}_i = \left(\boldsymbol{A}^{\mathrm{H}}\boldsymbol{A}\right)^{-1/2}\boldsymbol{A}^{\mathrm{H}}\boldsymbol{e}_i\boldsymbol{e}_i^{\mathrm{T}}\boldsymbol{A}\left(\boldsymbol{A}^{\mathrm{H}}\boldsymbol{A}\right)^{-1/2},$$

and $\boldsymbol{e}_i$ denotes the ith column of the $MM_t \times MM_t$ identity matrix. The differential $\mathrm{d}f_i$, computed at the point $\boldsymbol{s}_{(k)}$, is given by [24]

$$\mathrm{d}f_i = \left(d\boldsymbol{s}_{(k)}\right)^{\mathrm{H}}\widetilde{\boldsymbol{A}}_i\boldsymbol{s}_{(k)} + \boldsymbol{s}_{(k)}^{\mathrm{H}}\widetilde{\boldsymbol{A}}_i d\boldsymbol{s}_{(k)} = \Re\{(d\boldsymbol{s}_{(k)})^{\mathrm{H}}2\widetilde{\boldsymbol{A}}_i\boldsymbol{s}_{(k)}\}.$$

Now, it is straightforward to identify the gradient. Hence, the gradient is given by [24]

$$\nabla f_i\left(\boldsymbol{s}_{(k)}\right) = \begin{bmatrix} \Re\{2\widetilde{\boldsymbol{A}}_i\boldsymbol{s}_{(k)}\} \\ \Im\{2\widetilde{\boldsymbol{A}}_i\boldsymbol{s}_{(k)}\} \end{bmatrix}.$$

IET Commun., 2016, Vol. 10, Iss. 2, pp. 212–218